ISPRS Journal of Photogrammetry and Remote Sensing 74 (2012) 34–40

Contents lists available at SciVerse ScienceDirect

ISPRS Journal of Photogrammetry and Remote Sensing

journal homepage: www.elsevier.com/locate/isprsjprs

Mapping evergreen forests in the Brazilian Amazon using MODIS and PALSAR 500-m mosaic imagery

Sage Sheldon *, Xiangming Xiao, Chandrashekhar Biradar

Department of Botany and Microbiology, Center for Spatial Analysis, University of Oklahoma, Norman, OK 73019, USA

A R T I C L E I N F O

Article history:
Received 28 February 2011
Received in revised form 1 July 2012
Accepted 6 July 2012
Available online 23 September 2012

Keywords:
PALSAR/ALOS
MODIS
Radar
SAR
Amazonia
Brazil

A B S T R A C T

In this study, we evaluate a methodology that uses dual-polarization L-band SAR 500-m mosaic PALSAR imagery to identify and map forests in the Brazilian Amazon and an algorithm that uses time-series MODIS imagery to map evergreen forest. IKONOS images were used to evaluate forest maps derived from PALSAR and MODIS imagery. A comparison between the PALSAR forest map and IKONOS forest maps shows that 91.4% of PALSAR-derived forest pixels had greater than 60% IKONOS-derived forest area. We also compared the PALSAR-derived forest map with the MODIS-derived evergreen forest map. Out of 1999 evergreen forest pixels in the MODIS evergreen forest map (the areas covered by the 11 IKONOS imagery), 1934 pixels were identified as forest by the PALSAR forest map, approximately 96.7% agreement. The results of this study highlight the potential of combining PALSAR and MODIS data for identifying and mapping evergreen forests in the Amazon.

1. Introduction

The Amazon basin has the largest area of tropical rainforest in the world and may hold one-fourth of the world's biodiversity (Malhi et al., 2008). This region is undergoing deforestation at concerning rates. In addition to clear-cuts for timber production, deforestation for conversion to agricultural land, selective logging, degradation, and accidental fire also contribute to loss of forests in the region (Betts et al., 2008; Morton et al., 2006). The deforestation in the region poses threats to local and global climate stability (Betts et al., 2008). Information on the current state of tropical forest and the ability to monitor annual deforestation and regrowth in this region are needed to address scientific and political challenges.

Over the last few decades a number of studies have used images from optical sensors to map forests in the Amazon, including Landsat (Nelson et al., 1987; Skole and Tucker, 1993), Advanced Very High Resolution Radiometer (AVHRR) (Mayaux et al., 1998; Stone et al., 1991), Satellite Pour l'Observation de la Terre (SPOT)-4 VEGETATON (Carreiras and Pereira, 2005; Souza et al., 2003), and Moderate Resolution Imaging Spectroradiometer (MODIS) (Friedl et al., 2002; Hansen et al., 2008a; Wessels et al., 2004). MODIS and Landsat data were integrated to map forest cover and change in the humid tropical region (Hansen et al., 2008b) and in the Congo Basin (Hansen et al., 2008a). The spatial resolution (250 m to 1 km depending on the band) of MODIS data is low compared to other optical sensors (e.g., Landsat); however, MODIS data are collected for the entire Earth surface every 1–2 days in 36 spectral bands and can be more rapidly processed and analyzed than higher resolution remote sensing. Hansen et al. (2008a) compared Brazilian forest cover change estimates between a MODIS-derived estimation and deforestation data from the Amazon Deforestation Monitoring Project (PRODES). The 32-day MODIS composites and a decision tree algorithm were used to produce MODIS-derived change estimates that corresponded to 75% of the change in PRODES estimates (Hansen et al., 2008a). Frequent cloud cover in the moist tropic region often results in few good quality observations in a year, which constrains the capacity of optical sensors for monitoring tropical forests.

Synthetic Aperture Radar (SAR) provides cloud-free images. Studies have evaluated the use of C-band and L-band SAR imagery to map and monitor forests and concluded that L-band SAR has greater sensitivity to vegetation structure than other bands (C-band) (Grover et al., 1999; Luckman et al., 1997; Rosenqvist et al., 2004). Using L-band SAR from the Japanese Earth Resources Satellite (JERS-1), Angelis et al. (2002) found differences in radar backscatter between cleared land, regenerating forest, and primary forest. However, recent studies in the Brazilian Amazon by Almeida-Filho et al. (2005, 2007) demonstrated that single-polarization (HH) radar data from JERS-1 has limitations in detecting newly deforested areas.

The Advanced Land Observing Satellite (ALOS) with the Phased Array type L-band Synthetic Aperture Radar (PALSAR) was

* Corresponding author. Address: 3100 Monitor Ave., Suite 180, University of Oklahoma, Norman, OK 73072, USA. Tel.: +1 405 325 6076.
E-mail address: sage.sheldon@ou.edu (S. Sheldon).

0924-2716/$ - see front matter © 2012 International Society for Photogrammetry and Remote Sensing, Inc. (ISPRS) Published by Elsevier B.V. All rights reserved.
http://dx.doi.org/10.1016/j.isprsjprs.2012.07.003

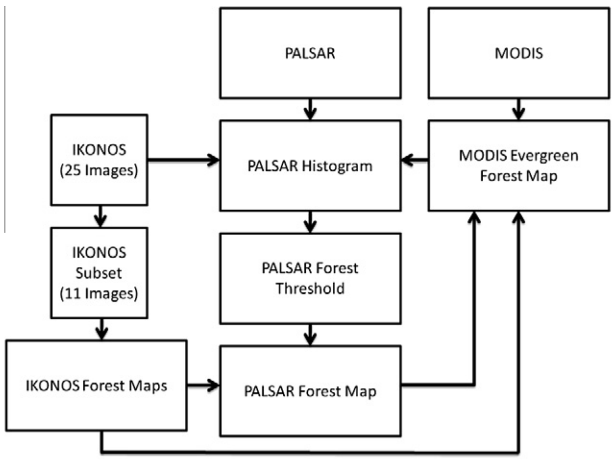

Fig. 1. A simple schematic workflow diagram of this study.

launched on January 24, 2006 by the Japan Aerospace Exploration Agency (JAXA). Several studies have evaluated the potential of dual-polarization L-band PALSAR for characterization of forests (Almeida-Filho et al., 2009; Fransson et al., 2007). A recent case study showed that 50-m resolution ALOS PALSAR data could be used to differentiate between primary forest and newly deforested areas in the Brazilian Amazon (Almeida-Filho et al., 2009). The 50-m resolution ALOS PALSAR Mosaic Product for the Amazon has not yet been released to the public, but the PALSAR 500-m Browse Mosaic Product for the Amazon is available. The freely available PALSAR 500-m mosaic products have two polarizations (HH and HV). For detailed information on the production of these data, see (Shimada et al., 2009, 2010).

PALSAR-based forest maps do not differentiate evergreen forests from deciduous forests or standing dead trees (e.g., fire disturbance). However, time series MODIS data could easily differentiate deciduous forests and evergreen forests. In this study, we explored the potential and benefits of combining SAR and MODIS imagery to map tropical forests. The objective of this study is twofold: (1) explore and evaluate the potential of the PALSAR 500-m mosaic product for identifying and mapping tropical forests in the Brazilian Amazon; (2) compare the PALSAR-based forest map with a MODIS-derived evergreen forest map, and evaluate the potential for monitoring evergreen forest using combined MODIS and PALSAR datasets (see Fig. 1).

2. The study site and data

2.1. The Brazilian Amazon study site

The Amazon basin was chosen as a study site because it is the world's largest continuous region of tropical rainforest and deforestation is the most direct and immediate danger to Amazon forests. Large-scale mechanized agriculture, such as beef and soy exportation, has been a major driver of deforestation in the Brazilian Amazon in recent years (Almeida-Filho et al., 2005; Morton et al., 2006). Until recently, deforestation mainly took place along the southeastern border of the Amazon but is now increasingly occurring in central Amazonia (Almeida-Filho et al., 2005; Shimada et al., 2009).

2.2. IKONOS image data in 2000 and 2001

The sun-synchronous, polar orbiting IKONOS satellite operated by Geo Eye acquires imagery in four spectral bands (blue, green, red, and near-infrared) at a 4-m spatial resolution and panchromatic band at 1-m spatial resolution. In 2000 and 2001, the Large-scale Biosphere–Atmosphere Experiment in Amazonia (LBA), under the support of NASA, acquired IKONOS imagery for 34 CO_2 flux tower sites and 56 intensive field study sites, covering a variety of terrestrial ecosystems in the Amazon (Hurtt et al., 2003). These images were selected during the LBA project such that they are geographically dispersed and cover a variety of ecosystems. From this IKONOS image database, we selected 25 geospatially dispersed scenes for initial quality screening. We selected IKONOS scenes with such criteria that they (1) clearly showed forest, agricultural land, deforested land, or water bodies; and (2) showed no change in forest coverage between 2001 and 2007 (the date of the earliest cycle of PALSAR data available), as verified by comparison with Google Earth imagery.

2.3. MODIS image data in 2007

The MODIS Land Science Team provides several surface reflectance data products, including the 8-day composite MODIS Land Surface Reflectance Product (MOD09A1). There are forty-six 8-day composites in a year. Each 8-day composite (MOD09A1) includes land surface reflectance for the seven spectral bands at 463-m spatial resolution: blue (459–479 nm), green (545–565 nm), red (620–670 nm), near infrared (841–875 nm, 1230–1250 nm), and shortwave infrared (1628–1652 nm, 2105–2155 nm). The MOD09A1 data files (collection 5, http://modis-sr.ltdri.org/; accessed 01 June 2012) provide data quality flags to indicate poor observations due to cloud interference, cloud shadow, aerosols, and pixels adjacent to clouds. We excluded those observations with the above-mentioned quality flags from statistical data analysis. Additionally, those observations with a blue band value >0.20 were excluded from statistical data analysis because high reflectance values in the blue band indicate atmospheric contamination (e.g., from smoke or thin clouds) resulting in poor quality observations (Xiao et al., 2005a).

We calculated three vegetation indices: Normalized Difference Vegetation Index (NDVI) (Tucker, 1979), Enhanced Vegetation Index (EVI) (Huete et al., 1997), and Land Surface Water Index (LSWI) (Xiao et al., 2002), using blue, red, NIR_1 (841–875 nm) and $SWIR_2$ (1628–1652 nm) spectral bands. The resultant vegetation indices are available at the Earth Observation and Modeling Facility web site (http://www.eomf.ou.edu; accessed 01 June 2012). The LSWI and EVI vegetation indices are related to leaf area index, canopy chlorophyll and water content (Xiao et al., 2005b). Using these vegetation indices and a mapping algorithm, we produced a MODIS-derived evergreen forest map for the Amazon Basin as described in Methods Section 3.2.

2.4. ALOS PALSAR 500-m mosaic data product in 2007

The PALSAR 500-m browse mosaic product covers the entire world (http://www.eorc.jaxa.jp/ALOS/en/about/palsar.htm; accessed 01 June 2012) and is generated for every PALSAR data acquisition cycle. The South America PALSAR 500-m mosaic data from cycles 12 (June 7–July 22, 2007) and 14 (September 07–October 22, 2007) with dual polarizations HH and HV were used in this study (Rosenqvist et al., 2007; Shimada et al., 2009). These acquisition cycles were chosen because they are the earliest PALSAR cycles available and closest in time to the IKONOS images used in this study for algorithm development and validation. Multiple swaths of data are missing for 2007 even after mosaicking Cycle 12 and Cycle 14; however, most of the study region has PALSAR coverage.

We converted PALSAR data (Cycles 12 and 14, HH and HV) from amplitude (DN) to normalized radar cross section (NRCS, σ^0) using the equation and the calibration factor given by JAXA in the ALOS/

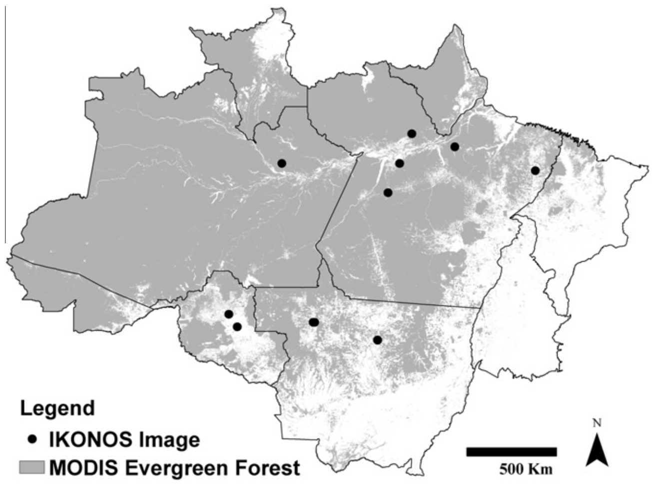

Fig. 2. IKONOS locations and the 2007 MODIS evergreen forest map. The locations of IKONOS images used to evaluate forest mapping algorithms in this study are shown with the MODIS-derived evergreen forest map for 2007.

PALSAR Mosaic Product Format Description Document (Rosenqvist et al., 2007; Shimada et al., 2009):

$$\sigma^0 = 10 * \log_{10}\langle DN^2 \rangle + CF \tag{1}$$

where σ^0 is the backscattering coefficient (normalized radar cross section), DN is the digital number, and CF is the calibration factor provided by JAXA (−83 for these data). We also calculated the HH/HV ratio for Cycles 12 and 14. Even after normalizing the radar data, the PALSAR 2007 data had some spurious values between swaths, a problem occurring only in PALSAR 500-m mosaic data in 2007.

3. Methods

3.1. Mapping forests with IKONOS images

In order to assess the PALSAR forest map, a second subset of 11 IKONOS images (see Fig. 2) representing the range of both Amazonian forest and deforestation patches, as well as a range of PALSAR values (see Fig. 3), were selected to determine the efficacy of the PALSAR forest mapping thresholds because they were completely free of cloud cover. There was a time difference of 5–6 years between the IKONOS images and the PALSAR data used in this study. To ensure these images represent current forest extents, each IKONOS image was checked with Google Earth high-resolution imagery obtained around the dates of 2007 PALSAR data (see Fig. 4a and b). The extent of forests in each of the IKONOS images selected has remained static or had little change.

After stacking the red, green, and blue bands, we used the ERDAS Imagine ISODATA classification algorithm to perform a spectral interpretation and produce eight spectral classes for each IKONOS image. Visual interpretation and supervision was then combined with the classification process to produce a forest/non-forest classification of each IKONOS image. Fig. 4 shows an example of one of the most complex classified IKONOS multispectral images (Fig. 4a), a more recent high resolution Google Earth image – in this case October 7, 2009 (Fig. 4b), an overlay of the MODIS evergreen forest map (Fig. 4c), and an overlay of the PALSAR forest map (Fig. 4d).

The IKONOS-based forest maps have a spatial resolution of 4 m. To compare the IKONOS-derived forest maps with the PALSAR-derived forest map, a fishnet grid of cells was created for the exact locations of the 500-m PALSAR cells covered by the 11 IKONOS images. The Zonal Statistics function in ESRI's ArcMap software was used to provide estimates of the percentages of IKONOS-derived forest cells within each grid cell corresponding to PALSAR cells. This provides a quantification of the percentage of 4-m forest cells within each PALSAR forest/non-forest pixel (see Fig. 5a). This also provides information as to what percentage of forest structure within a 500-m area results in a PALSAR-derived forest classification according to this decision tree algorithm. The same methodology was used to calculate the percentage of forest (as derived from IKONOS) within each MODIS forest/non-forest pixel (see Fig. 5b). We then calculated the percentage of IKONOS-derived forest within MODIS forest pixels only (see Fig. 6b).

3.2. Mapping evergreen forests with MODIS

Xiao et al. (2009) recently developed a simple and novel algorithm to map evergreen forests and produce a map of evergreen forests in the pan-tropical zone in 2000 using MODIS data. This algorithm is based on temporal profile analysis of LSWI in a year and generates a map of evergreen forest (Xiao et al., 2009). In this study, we applied the same algorithm to MODIS data in 2007 and generated a map of evergreen forest in the Brazilian Amazon in 2007.

3.3. Mapping forests with PALSAR

For a first approximation of forest threshold ranges, we overlaid each PALSAR image (HH, HV, HH/HV ratio) with the MODIS forest map, and calculated frequency distributions of PALSAR backscatter values for HH, HV, and HH/HV across forests. The

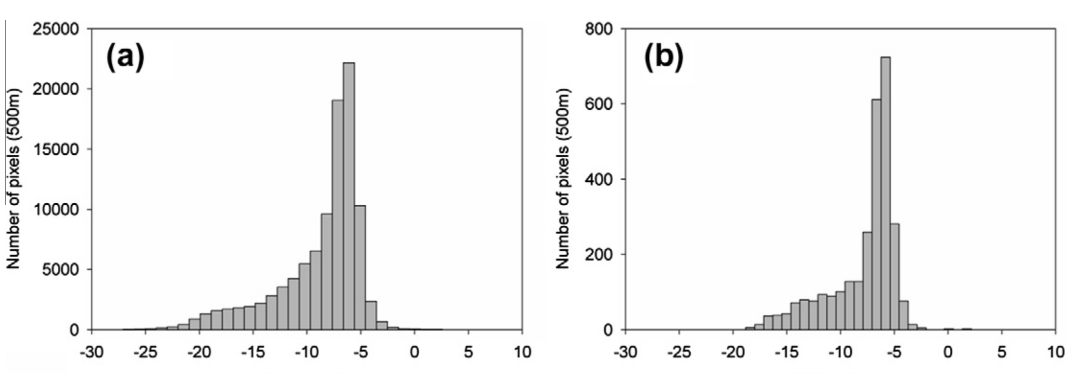

Fig. 3. A comparison between histograms of radar backscatters from PALSAR 500 m mosaic images in (a) Brazilian Amazon and (b) the areas with IKONOS images. This shows that the IKONOS subset has a similar distribution to the Brazilian Amazon as a whole.

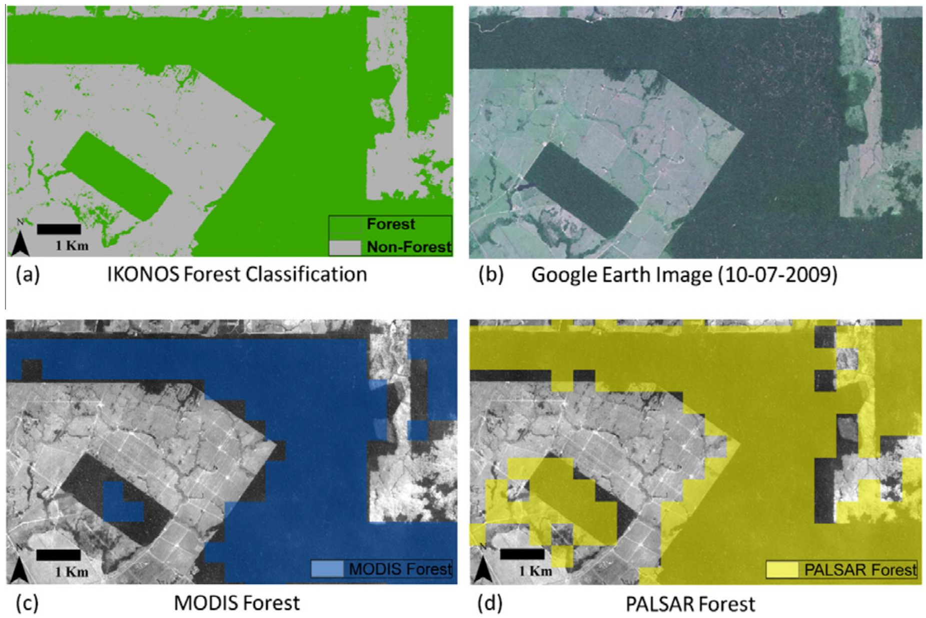

Fig. 4. From one of the most complex IKONOS imagery locations used in this study: (a) an IKONOS-derived forest map, (b) the corresponding Google Earth image on 10-07-2009 located at 10°08′00.93″S 62°44′11.37″W, (c) the MODIS-derived forest map and (d) the PALSAR-based forest map. Each IKONOS image from 2001 was checked in Google Earth (b) to make sure there were no changes in forest cover between 2001 and 2007 (the date of PALSAR data). We then classified forest/non-forest in each IKONOS image (a) and compared with the MODIS-derived forest map (c) and PALSAR-derived forest map (d).

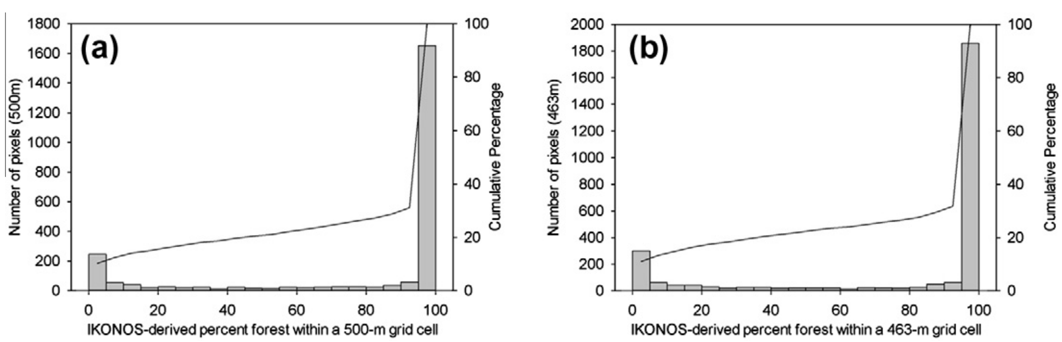

Fig. 5. A comparison between histograms and cumulative percentage of IKONOS-derived forest within each (a) 500-m PALSAR cell and (b) 463-m MODIS cell in the study area.

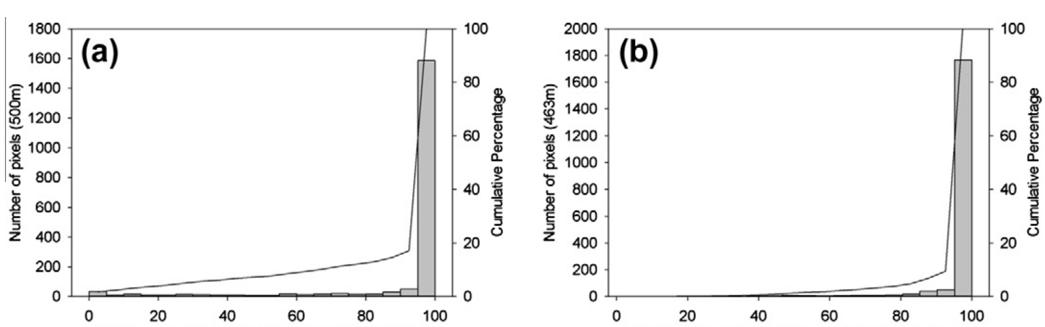

Fig. 6. A comparison between histograms and the cumulative percentage of IKONOS-derived forest within each (a) 500-m PALSAR-derived forest cell and (b) 463-m MODIS-derived forest cell.

histograms of HH, HV and HH/HV provide a visual graph for selecting a set of threshold ranges of forests. Using the tentative ranges of values for each polarization (HH and HV) and HH/HV ratio, we used a decision tree procedure to produce an initial set of PALSAR-derived forest maps. In order for a pixel to be classified as "forest," the values of HH, HV, and HH/HV backscatter at that location all had to fall within the threshold range for HH, HV or ratio.

We used IKONOS 4-m multispectral imagery to visually explore potential ranges of radar backscatter indicated by forest structure and determine the threshold range for forest. The threshold algorithm to reveal and determine forest structure is:

$$\text{Forest} = \begin{array}{l} -10.3 \leqslant HH \leqslant -1.8 \\ -19.5 \leqslant HV \leqslant -10.8 \\ 0.14 \leqslant HH/HV \leqslant 0.71 \end{array} \quad (2)$$

The HH backscatter threshold for forests is higher than the HV polarization. If the thresholds are set too high, then urban land cover will be classified as forest; alternatively, if the thresholds are set too low then agricultural land will be misclassified as forest.

For visual interpretation and comparison, the initial PALSAR forest maps were overlaid with 25 false color composite IKONOS images, which allowed for the clear selection of one set of PALSAR value ranges for forests. We overlaid the IKONOS images with HH, HV and HH/HV ratio images, and calculated frequency distributions of HH, HV and HH/HV ratio for those PALSAR pixels within the areas covered by the IKONOS images (Fig. 3). The histograms of HH, HV, and HH/HV ratio from this subset of PALSAR data have similar shapes and ranges as those of PALSAR pixels over the entire Brazilian Amazon basin (see Fig. 3). Distribution and range in backscatter values between this subset of IKONOS images and the entire Brazilian Amazon, shown in the HH histograms in Fig. 3, further indicate that the subset of PALSAR data in those areas covered by the IKONOS images are a representative sample of the Amazon Basin.

4. Results

4.1. MODIS forest map

Fig. 5b shows a cumulative histogram of the percentage of IKONOS-derived forest cover from all 11 IKONOS images within all MODIS pixels (forest/non-forest). Fig. 6b displays the cumulative histogram of the percentage of IKONOS-derived forest pixels for MODIS forest pixels only. A comparison of these data demonstrates that while a range of percentages of IKONOS forest cells exist within the 11 IKONOS images, the MODIS forest algorithm produces forest maps with pixels of higher percentages of IKONOS forest cells. Fig. 6b shows that the vast majority of MODIS-derived forest pixels have greater than 70% of forest area as determined by IKONOS imagery. Out of 1952 evergreen forest pixel comparisons, 1901 pixels (97.4%) classified as forest had 70% or more IKONOS-derived forest cover, 1932 pixels (99.0%) had greater than 50% cover, and 1948 pixels (99.8%) had greater than 30% forest cover.

4.2. PALSAR forest map

Using the locations of PALSAR 500-m pixels that correspond to the IKONOS images and the forest classification IKONOS images, we calculated the number of 4-m IKONOS forest pixels within each corresponding PALSAR pixel (see Figs. 5 and 6). This allowed for an analysis of the percentage of IKONOS forest pixels within each 500-m PALSAR pixel identified as either forest or non-forest. At 4-m resolution, IKONOS serves as ground truth for the area of forest within each 500-m pixel. Fig. 5a shows the percentage of IKONOS-derived forest cover from all 11 IKONOS images within both forest and non-forest PALSAR pixels. Fig. 6a shows the percentage of IKONOS forest pixels within PALSAR forest pixels only. These figures demonstrate that most PALSAR-based forest pixels have high percentages of IKONOS forest pixels. Unlike the MODIS evergreen forest map (Fig. 6b), the PALSAR forest map has a small number of pixels with percentage of forest below 40%. This could be due to recent deforestation where woody material remaining on the ground or remnant forest structure affects the backscatter (e.g., standing dead trees after a fire). The MODIS mapping algorithm would not recognize recent deforestation or remnant trees as forest because it is based on leaf area index, canopy chlorophyll, and water content. However, the vast majority of PALSAR-derived forest pixels have greater than 70% forest area as determined by IKONOS imagery. Out of 1916 pixels at 500-m resolution (as defined by 11 IKONOS images), 1721 pixels (89.8%) had 70% or more IKONOS-derived forest cover, 1778 pixels (92.8%) had greater than 50% cover, and 1821 pixels (95%) had greater than 30% forest cover.

4.3. Comparison between PALSAR forest map and MODIS forest map

MODIS pixels have an approximate resolution of 463-m while PALSAR pixels are at 500-m resolution. In order to compare the two datasets, the PALSAR-derived forest map was first resampled to 463-m resolution using the nearest neighbor algorithm, a standard methodology for converting remote sensing datasets to a similar resolution. Pixels from the PALSAR forest map and MODIS evergreen forest map that fell within the areas covered by the IKONOS imagery subset were compared with each other in order to evaluate the agreement between the two forest maps. A regional comparison between the PALSAR forest map and MODIS forest map was also performed to check the agreement between the two maps and satellite sensor types. For each MODIS evergreen forest pixel, the PALSAR classification – forest or non-forest – was extracted from an overlay process. As the MODIS algorithm maps only evergreen forest, we also determined the MODIS forest/non-forest classification for all PALSAR forest pixels but expected a lower percentage of pixel agreement since PALSAR detects forest structure and will include deciduous forest in addition to evergreen forest.

We co-registered the PALSAR forest map (resampling to 463 m resolution), MODIS evergreen forest map, and IKONOS forest maps (11 IKONOS images), and compared the PALSAR forest map and the MODIS evergreen forest map within the areas defined by the IKONOS images (a total of 2776 pixels at MODIS 463 m resolution). Out of the 1999 evergreen forest pixels in the MODIS evergreen forest map, 1934 pixels were identified as forest by the PALSAR forest map, resulting in 96.7% agreement. Out of 2186 forest pixels in the PALSAR-derived forest map, 1934 pixels were identified as evergreen forest by the MODIS evergreen forest, demonstrating 88.5% agreement. This relatively lower estimate of agreement may be to some degree attributed to the fact that the PALSAR-derived forest map includes evergreen forest and deciduous forest, whereas the MODIS algorithm used in this study maps evergreen forest only. In addition, the PALSAR-derived forest map could also include some land with standing dead trees after disturbance (e.g., due to fire).

At the regional scale, we overlaid the 463-m resolution PALSAR-derived forest map with the 463-m resolution MODIS-derived evergreen forest map for the area identified by MODIS as evergreen forest. We calculated the histograms of HH polarization values of PALSAR images from the forest pixels in the PALSAR forest map and in the MODIS evergreen forest map. The frequency distribution of HH polarization values from PALSAR in PALSAR-derived forest pixels (Fig. 7a) is very similar in both range and distribution to that of MODIS-derived evergreen forest pixels (Fig. 7b). After excluding the missing swaths of the PALSAR images, there are 20,055,180 pixels from PALSAR data and 24,150,543 total pixels from MODIS for the Brazilian Amazon. PALSAR identified 15,703,098 (78.3%) pixels as forest. MODIS identified 16,274,617 (67.4%) as evergreen forest pixels. Out of the 13,703,765 MODIS identified evergreen forest pixels that overlay with PALSAR pixels, 13,057,379 pixels were identified as forest by the PALSAR forest map, demonstrating 95.3% agreement.

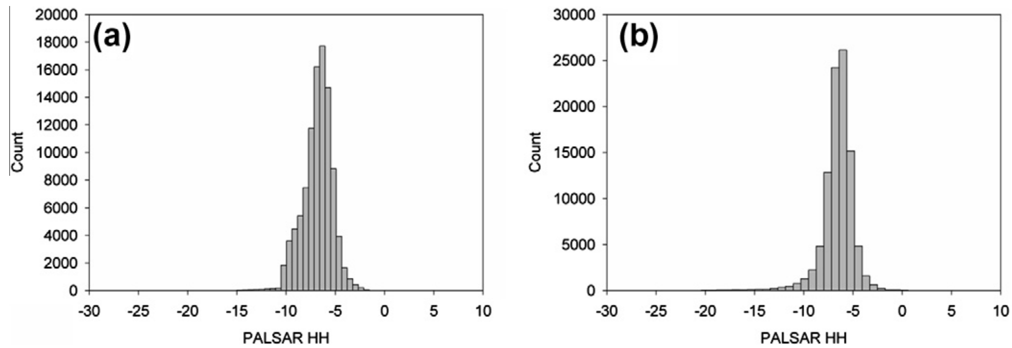

Fig. 7. A comparison between histograms of PALSAR HH radar backscatter values in (a) PALSAR-derived forest pixels and (b) MODIS-derived evergreen forest pixels.

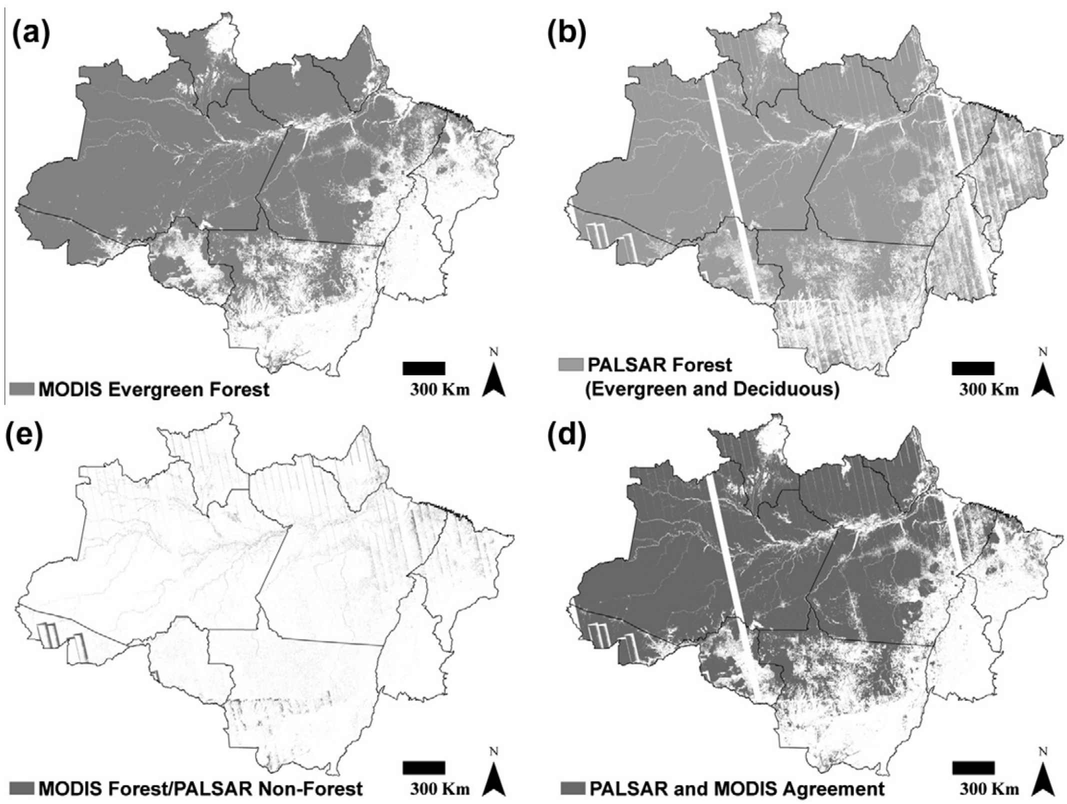

Fig. 8. A spatial comparison between the MODIS evergreen forest map and PALSAR forest map. The MODIS forest map (a) is derived from an algorithm that maps only evergreen forest in the Amazon Basin, whereas the PALSAR forest map (b) is based on radar imagery that maps both deciduous and evergreen forest. Using only the evergreen portion of the basin we compared the MODIS and PALSAR forest maps to determine their disagreement (c) and agreement (d).

The PALSAR forest map includes deciduous forests in the Cerrado region of Brazil (Fig. 8b) and the MODIS algorithm maps only evergreen forest (Fig. 8a); thus, the regional comparison between MODIS and PALSAR forest maps was carried out for evergreen forest only. Fig. 8c shows the pixels mapped as evergreen forest by the MODIS algorithm but as non-forest by PALSAR. Some of these pixels are along rivers where the MODIS algorithm identified a small number of water pixels as forest. The rest of the disagreement results from the portion of the 2007 cycle that had spurious values along swaths even after calibration and normalization. Fig. 8d provides a map of pixels classified to be forest by both the PALSAR forest and MODIS evergreen forest algorithms. This map demonstrates the agreement between two very different sensors and algorithms. The combination of the PALSAR-based forest map and MODIS-based evergreen forest map generates a new evergreen forest map in Brazilian Amazon, based on spectral properties from optical remote sensing and structural properties from L-band SAR.

5. Discussion and conclusion

To our knowledge, this is the first study evaluating the potential of large-scale forest mapping and monitoring in the Brazilian Amazon using PALSAR 500-m mosaic data. The comparison between a MODIS-derived evergreen forest map and a PALSAR-derived forest map shows strong agreement between the two algorithms and sensors: the PALSAR-derived forest map shows a 95.3% agreement with MODIS-derived evergreen forest pixels. The combination of PALSAR and MODIS allows for more complete coverage and confidence in estimates. The International Geosphere–Biosphere Program (IGBP) defines evergreen broadleaf forests as lands with greater than 60% cover by woody vegetation (Giri et al., 2005). Out of the PALSAR pixels evaluated, 89.8% classified as forest showed greater than 70% IKONOS-derived forest area and 91.4% of PALSAR-derived forest pixels had greater than 60% IKONOS-derived forest area.

Some PALSAR-derived forest pixels showed tree structure in the IKONOS imagery, and yet one of the polarizations did not return a backscatter value within its forest threshold range (HH −10.3 to −1.8, HV −19.5 to −10.8, and HH/HV 0.14–0.71). Thus, in a small percentage of pixels, the orientation, amount, or height of woody biomass does not result in HH, HV, and HH/HV backscatter falling within the forest threshold. Almeida-Filho et al. (2007) demonstrated that in cases where newly deforested areas retain stems and other woody material, newly deforested areas can display greater radar backscatter than primary forest. Future work should be aimed at further investigation of radar returns for newly deforested areas with remnant woody structure.

Despite these challenges, multiple cycles from PALSAR over a year and the straightforward methodology evaluated here, combined with the MODIS evergreen forest mapping algorithm, provide a way to monitor Amazonian and potentially other tropical forests annually. A yearly 500-m PALSAR-derived forest map can be combined with a 463-m MODIS-derived evergreen forest map for identifying and mapping both deciduous forests and evergreen forests. Furthermore, the combination of PALSAR and MODIS imagery, as shown in this study, may offer a new opportunity and tool to track both deforestation and re-forestation, which will improve our capacity to better quantify forests in the Amazon region.

Acknowledgments

This study was supported in part by a Grant from NASA Land Use and Land Cover Change Program (NNX09Ac39G), a Grant from National Institutes of Health through the NSF/NIH Ecology of Infectious Diseases Program (R01-TW007869), a Grant from the National Science Foundation (NSF) EPSCoR Program (NSF-0919466), and the faculty start-up Grant to Dr. Xiangming Xiao at the University of Oklahoma. We thank the reviewers for their valuable comments and suggestions on the earlier version of the manuscript.

References

Almeida-Filho, R., Roskenqvist, A., Shimabukuro, Y.E., dos Santos, J.R., 2005. Evaluation and perspectives of using multitemporal L-band SAR data to monitor deforestation in the Brazilian Amazonia. IEEE Geoscience and Remote Sensing Letters 2 (4), 409–412.

Almeida-Filho, R., Rosenqvist, A., Shimabukuro, Y.E., Silva-Gomez, R., 2007. Detecting deforestation with multitemporal L-band SAR imagery: a case study in western Brazilian Amazonia. International Journal of Remote Sensing 28 (6), 1383–1390.

Almeida-Filho, R., Rosenqvist, A., Shimabukuro, Y.E., Silva-Gomez, R., 2007. Detecting deforestation with multitemporal L-band SAR imagery: a case study in western Brazilian Amazonia. International Journal of Remote Sensing 28 (6), 1383–1390.

Almeida-Filho, R., Shimabukuro, Y.E., Rosenqvist, Al., Sanchez, G.A., 2009. Using dual-polarized ALOS PALSAR data for detecting new fronts of deforestation in the Brazilian Amazonia. International Journal of Remote Sensing 30 (14), 3735–3743.

Angelis, C.F., Freitas, C.C., Valeriano, D.M., Dutra, L.V., 2002. Multitemporal analysis of land use/land cover JERS-1 backscatter in the Brazilian tropical rainforest. International Journal of Remote Sensing 23 (7), 1231–1240.

Betts, R.A., Malhi, Y., Roberts, J.T., 2008. The future of the Amazon: new perspectives from climate, ecosystem and social sciences. Philosophical Transactions of the Royal Society B – Biological Sciences 363 (1498), 1729–1735.

Carreiras, J.M.B., Pereira, J.M.C., 2005. SPOT-4 VEGETATION multi-temporal compositing for land cover change studies over tropical regions. International Journal of Remote Sensing 26 (7), 1323–1346.

Fransson, J.E.S., Magnusson, M., Olsson, H., Eriksson, L.E.B., Sandberg, G., Smith-Jonforsen, G. Ulander, L.M.H., 2007. Detection of forest changes using ALOS PALSAR satellite images. In: Geoscience and Remote Sensing Symposium 2007, IGARSS, IEEE International, Barcelona, Spain, 23–28 July, pp. 2330–2333.

Friedl, M.A., McIver, D.K., Hodges, J.C.F., Zhang, X.Y., Muchoney, D., Strahler, A.H., Woodcock, C.E., Gopal, S., Schneider, A., Cooper, A., Baccini, A., Gao, F., Schaaf, C., 2002. Global land cover mapping from MODIS: algorithms and early results. Remote Sensing of Environment 83 (1–2), 287–302.

Giri, C., Zhu, Z., Reed, B., 2005. A comparative analysis of the Global Land Cover 2000 and MODIS land cover data sets. Remote Sensing of Environment 94 (1), 123–132.

Grover, K., Quegan, S., Freitas, C.D., 1999. Quantitative estimation of tropical forest cover by SAR. IEEE Transactions on Geoscience and Remote Sensing 37 (1), 479–490.

Hansen, M.C., Shimabukuro, Y.E., Potapov, P., Pittman, K., 2008a. Comparing annual MODIS and PRODES forest cover change data for advancing monitoring of Brazilian forest cover. Remote Sensing of Environment 112 (10), 3784–3793.

Hansen, M.C., Stehman, V., Potapov, P., Loveland, T.R., Townshend, J.R., DeFries, R.S., Pittman, K., Arunarwati, B., Stolle, F., Steininger, M., Carroll, M., DiMiceli, C., 2008b. Humid tropical forest clearing from 2000 to 2005 quantified by using multitemporal and multiresolution remotely sensed data. Proceedings of the National Academy of Sciences of the United States of America 105 (27), 9439–9444.

Huete, A.R., Liu, H.Q., Batchily, K., vanLeeuwen, W., 1997. A comparison of vegetation indices over a global set of TM images for EOS-MODIS. Remote Sensing of Environment 59 (3), 440–451.

Hurtt, G., Xiao, X., Keller, M., Palace, M., Asner, G.P., Braswell, R., Brondizio, E.S., Cardoso, M., Carvalho, C., Fearon, M.G., Guild, L., Hagen, S., Hetrick, S., Moore, B., Nobre, C., Read, J.M., Sa, T., Schloss, A., Vourlitis, G., Wickel, A.J., 2003. IKONOS imagery for the Large Scale Biosphere–Atmosphere Experiment in Amazonia (LBA). Remote Sensing of Environment 88 (1–2), 111–127.

Luckman, A., Baker, J., Kuplich, T.M., Yanasse, C.D.F., Frery, A.C., 1997. A study of the relationship between radar backscatter and regenerating tropical forest biomass for spaceborne SAR instruments. Remote Sensing of Environment 60 (1), 1–13.

Malhi, Y., Roberts, J.T., Betts, R.A., Killeen, T.J., Li, W.H., Nobre, C.A., 2008. Climate change, deforestation, and the fate of the Amazon. Science 319 (5860), 169–172.

Mayaux, P., Achard, F.R., Malingreau, J.-P., 1998. Global tropical forest area measurements derived from coarse resolution satellite imagery: a comparison with other approaches. Environmental Conservation 25 (1), 37–52.

Morton, D., DeFries, R., Shimabukuro, Y.E., Anderson, L.O., Arai, E., Espirito-Santo, F., Freitas, R., Morisette, J., 2006. Cropland expansion changes deforestation dynamics in the southern Brazilian Amazon. Proceedings of the National Academy of Sciences of the United States of America 103 (39), 14637–14641.

Nelson, R., Horning, N., Stone, T.A., 1987. Determining the rate of forest conversion in Mato Grosso, Brazil, using Landsat MSS and AVHRR data. International Journal of Remote Sensing 8 (12), 1767–1784.

Rosenqvist, A., Shimada, M., Ito, N., Watanabe, M., 2007. ALOS PALSAR: a pathfinder mission for global-scale monitoring of the environment. IEEE Transactions on Geoscience and Remote Sensing 45 (11), 3307–3316.

Rosenqvist, A., Shimada, M., Chapman, B., McDonald, K., De Grandi, G., Jonsson, H., Williams, C., Rauste, Y., Nilsson, M., Sango, D., Matsumoto, M., 2004. An overview of the JERS-1 SAR Global Boreal Forest Mapping (GBFM) project. In: Geoscience and Remote Sensing Symposium, IGARSS, IEE International, Tokyo, Japan, 20–24 September, pp. 1033–1036.

Shimada, M., Tadono, T., Rosenqvist, A., 2010. Advanced Land Observing Satellite (ALOS) and monitoring global environmental change. Proceedings of the IEEE 98 (5), 780–799.

Shimada, M., Isoguchi, O., Tadono, T., Isono, K., 2009. PALSAR Radiometric and Geometric Calibration. IEEE Transactions on Geoscience and Remote Sensing 47 (12), 3915–3932.

Skole, D., Tucker, C., 1993. Tropical deforestation and habitat fragmentation in the Amazon: satellite data from 1978 to 1988. Science 260 (5116), 1905–1910.

Souza, C., Firestone, L., Silva, L.M., Roberts, D., 2003. Mapping forest degradation in the Eastern Amazon from SPOT 4 through spectral mixture models. Remote Sensing of Environment 87 (4), 494–506.

Stone, T.A., Brown, I.F., Woodwell, G.M., 1991. Estimation, by remote sensing, of deforestation in central Rondonia, Brazil. Forest Ecology and Management 38 (3–4), 291–304.

Tucker, C.J., 1979. Red and photographic infrared linear combinations for monitoring vegetation. Remote Sensing of Environment 8 (2), 127–150.

Wessels, K.J., DeFries, R., Dempewolf, J., Anderson, L., Hansen, A.J., Powell, S.L., Moran, E., 2004. Mapping regional land cover with MODIS data for biological conservation: examples from the greater yellostone ecosystem, USA and Para State, Brazil. Remote Sensing of Environment 92 (1), 67–83.

Xiao, X., Biradar, C., Czarnecki, C., Alabi, T., Keller, M., 2009. A simple algorithm for large-scale mapping of evergreen forests in tropical America, Africa, and Asia. Remote Sensing 1 (3), 355–374.

Xiao, X., Boles, S., Frolking, S., Salas, W., Moore, B., Li, C., He, L., Zhao, R., 2002. Observation of flooding and rice transplanting of paddy rice fields at the site to landscape scales in China using VEGETATION sensor data. International Journal of Remote Sensing 23 (15), 3009–3022.

Xiao, X., Zhang, Q., Hollinger, D., Aber, J., Moore, B., 2005a. Modeling gross primary production of an evergreen needleleaf forest using MODIS and climate data. Ecological Applications 15 (3), 954–969.

Xiao, X., Boles, S., Liu, J.Y., Zhuang, D.F., Frolking, S., Li, C.S., Salas, W., Moore, B., 2005b. Mapping paddy rice agriculture in southern China using multi-temporal MODIS images. Remote Sensing of Environment 95 (4), 480–492.